Wireless Controlled Local Heating and Mixing Multiple Droplets Using Micro-Fabricated Resonator Array for Micro-Reactor Applications

ZHAN WANG[iD]**, HONGXIANG ZHANG, YANG YANG, HEMI QU, ZIYU HAN, WEI PANG, AND XUEXIN DUAN**[iD]

State Key Laboratory of Precision Measuring Technology and Instruments, Tianjin University, Tianjin 300072, China

Corresponding author: Xuexin Duan (xduan@tju.edu.cn)

ABSTRACT This paper reported a wireless controlled micro-actuator system for rapid heating and mixing of multiple droplets using integrated arrays of micro-fabricated 2.5 GHz solid-mounted thin-film piezoelectric resonators (SMRs) and a millimeter-scale omnidirectional antenna. An equivalent circuit is proposed to analyze the mechanism of the heating, mixing of the SMR, and the wireless communication system. The heating and mixing rate can be tuned by adjusting the input power as well as the transmission distance between the transmitting antenna and the receiving antennas. A heating rate up to 3.7 °C per second and ultra-fast mixing of the droplet was demonstrated with the wireless microsystem. In addition, two types of circuits, H-shaped and rake-shaped, were designed and fabricated for parallel operating actuator array and controlling the power distribution with the array. Both uniform and gradient heating of the multiple droplets are achieved, which can be potentially applied for developing high-throughput wireless micro-reactor system.

INDEX TERMS Chemical reactors, piezoelectric actuators, wireless communication.

I. INTRODUCTION

Developing droplet micro-reactors are of great interests for a variety of (bio)chemical applications such as drug discovery [1], [2], biomedical assay [3], combinatorial chemistry [4], and other lab-on-chip applications [5]–[8]. Because of the limited volume, high efficient heating and mixing in such small droplet is rather challenging. Micro-fabricated heater [9], [10] and mixer [11], [12], as well as their integrations [13], have been developed for this end. Acoustic resonators are reported as one of the represented active actuators to heat the droplets [14], [15] due to the dissipation of the acoustic energy into the liquid. In a recent work, we have demonstrated the rapid heating and mixing in liquid droplets using a MEMS fabricated solid-mounted film bulk acoustic resonator (SMR) [13], [16] which has a clear advantage of CMOS compatibility, high effective electromechanical coupling, high solution stability, and is able to generating micro-vortices at device-liquid interface to enhance the droplet mixing [17]–[19].

Most of the existing micro-reactor system uses wire connections from the devices to the external power source.

However, when it comes to harsh or closed environment, as well as narrow space, the conventional wired connections are limited. In addition, for developing high-throughput micro-reactors, manipulation of multiple droplets is required [20]–[22]. For these reasons, there has been growing interests in developing wireless heating techniques. Microwave [9], [23], induction [24], and LC circuit heating [25], [26] have been reported so far. However, these methods have various practical challenges, including long-distance control, limited to certain types of liquid, hard for minimization or implantation, and unable to heat individual droplet. The methods of microwave and induction heating are hard to achieve arrays. And all of these methods cannot achieve wireless mixing of droplets. Thus, developing wireless driven micro-devices for developing high throughput droplet micro-reactors is on strong demand. Furthermore, to the author's knowledge, wireless controlled local heating and mixing multiple droplets has been rarely reported.

In this work, we developed a novel wireless controlled micro-reactor system for high throughput heating and mixing multiple droplets by integrating arrays of SMRs with a

millimeter-scale omnidirectional antenna on a single PCB board. The resonator is powered by electromagnetic-field coupling, thus no hard wire, energy storage or harvesting components are required. An equivalent circuit of the wireless system is proposed to explain the mechanism of electromagnetic-field coupling. Wireless passive heating and mixing of 1 μl water droplet is experimentally demonstrated. The heating and mixing rate are studied with different powers applied to the transmitting antenna as well as the transmission distance between transmitting and receiving antennas. Uniform and gradient heating of multiple droplets were achieved by using two types of circuits, H-shaped and raked-shaped, which proves another advantage of using wireless techniques.
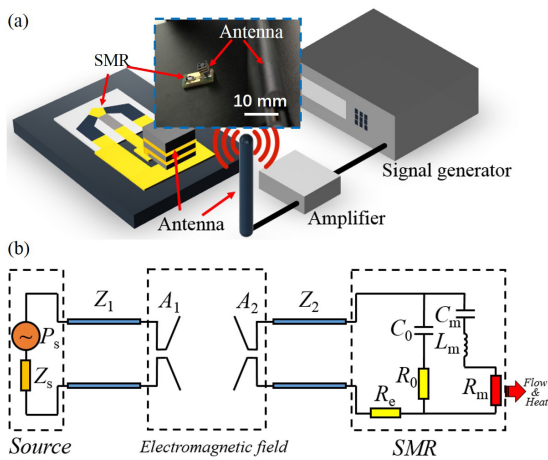
FIGURE 1. (a) Schematic diagram of the wireless controlled SMR as actuator for heating and mixing of microscale droplet. The inset is an image of the device. (b) The equivalent circuit model of wireless passive actuation.

II. WIRELESS MICRO-REACTOR DESIGN

A. EXPERIMENTAL SETUP

The schematic diagram of the experimental setup for wireless droplet heating and mixing is shown in Figure 1 (a). A solid mounted resonator (SMR) with a resonant frequency of 2.50 GHz and millimeter-scale omnidirectional receiving antenna (Molex, 047980001) were integrated on a single PCB board. The PCB is fabricated with FR-4 epoxy glass substrate. The substrate dielectric constant is 4.5 and the thickness of PCB is 1.6 mm. A commercial monopolar antenna was connected to RF signal generator (Agilent EXG Analog Signal Generator N5171B) and power amplifier (MODEL NO. ZHL-5W-422+) as a transmitting antenna. Wireless passive actuation of SMR was achieved via electromagnetic-field coupling between transmitting and receiving antennas. The illustration of SMR is shown in Figure S3 in the supplementary material.

B. MECHANISM OF WIRELESS PASSIVE ACTUATION

The equivalent circuit model of the wireless passive actuator is shown in Figure 1(b), which composes the source circuit,

the electromagnetic field coupled circuit and the Butterworth Van Dyke (BVD) equivalent circuit of SMR. P_s and Z_s refer to the input power and input impedance. Z_1 and Z_2 refer to the characteristic impedance of coaxial transmission line, while A_1 and A_2 represent the transmitting antenna and receiving antenna, respectively. C_0, C_m and L_m represent the static capacitance, the motional capacitance and the motional inductance. R_e, R_0 and R_m represent the resistance of the metal electrodes, the resistance related to dielectric losses and the motional resistance associated with acoustic losses, respectively. The complex Poynting vector (S) of electric dipole can be decomposed into two parts: radial Poynting vector (S_r) and polar Poynting vector (S_θ),

$$S_r = \frac{\eta_0}{8} I_0^2 \left(\frac{l}{\lambda}\right)^2 \frac{\sin^2\theta}{r^2} \left[1 - j\left(\frac{1}{kr}\right)^3\right], \quad (1a)$$

$$S_\theta = j\eta_0 I_0^2 \frac{kl^2 \cos\theta \sin\theta}{16\pi^2 r^3} \left[1 + \left(\frac{1}{kr}\right)^2\right], \quad (1b)$$

Here, η_0, I_0, l, θ, λ and k represent the wave impedance in air, current amplitude of electric dipole, length of electric dipole, polar angle, wave length ($\sim$0.12 m calculated in air and $\sim$0.07 m in FR-4 at the resonance frequency of 2.5 GHz) and wave number. r refers to the distance between transmitting antenna and receiving antenna, indicating that the wireless actuation of SMR can be controlled by adjusting the transmission distance.

In the near field of the antenna ($kr < 1$), high-order term of $1/kr$ play a dominant role, then the equation (1) can be simplified as

$$S_r = -j\frac{\eta_0}{8} I_0^2 \left(\frac{l}{\lambda}\right)^2 \frac{\sin^2\theta}{r^2} \left(\frac{1}{kr}\right)^3 \Rightarrow S_r \propto -j\left(\frac{1}{r}\right)^5, \quad (2a)$$

$$S_\theta = j\eta_0 I_0^2 \frac{kl^2 \cos\theta \sin\theta}{16\pi^2 r^3} \left(\frac{1}{kr}\right)^2 \Rightarrow S_\theta \propto j\left(\frac{1}{r}\right)^5, \quad (2b)$$

In this condition, the power is oscillating between electromagnetic field and antenna and does not radiate. The received power (P_{rec}) of receiving antenna can be deduced as

$$P_{rec} = \oint_S \mathbf{S} \cdot d\mathbf{s} \Rightarrow P_{rec} \propto \frac{1}{r^5}. \quad (3)$$

In the far field ($kr > 1$), high-order term of $1/kr$ can be ignored, then the equation (1) can be simplified as

$$S_r = \frac{\eta_0}{8} I_0^2 \left(\frac{l}{\lambda}\right)^2 \frac{\sin^2\theta}{r^2} \Rightarrow S_r \propto \frac{1}{r^2}, \quad (4a)$$

$$S_\theta = 0, \quad (4b)$$

Thus, the received power (P_{rec}) of receiving antenna can be deduced as

$$P_{rec} = \oint_S \mathbf{S} \cdot d\mathbf{s} \Rightarrow P_{rec} \propto \frac{1}{r^2}. \quad (5)$$

In our wireless system, the transmitting frequency of antenna is 2.5 GHz. $r < 1.91$ cm is the near field of the antenna and $r > 1.91$ cm is the far field.

C. MECHANISM OF DROPLET HEATING AND MIXING

In the BVD equivalent circuit, Rm represents the load of the resonator, which refers to the liquid droplet. The mechanism of droplet heating and mixing is further analyzed in supplementary material. The heat generated by fluid flow of per unit mass can be written as

$$Q = \rho c_0 \beta v^2, \tag{6}$$

The heat conduction equation in the flow field is given by

$$\rho C_p \left(\frac{\partial T}{\partial t} + \overrightarrow{v} \cdot \nabla T \right) = k \nabla^2 T + Q, \tag{7}$$

Where ρ, c_0, β and v represent he density of the liquid, sound velocity in liquid, the attenuation coefficient and the vibration velocity of liquid. C_p and k are the isobaric heat capacity and the thermal conductivity.
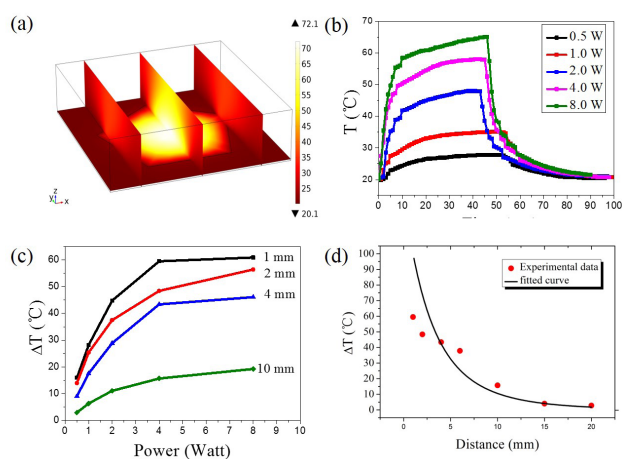
FIGURE 2. (a) COMSOL simulation of the energy conversion when SMR contacted with water, while the color gradient represents temperature distribution. **(b)** Temperature change of a 1 μl DI water droplet versus time with different input power, from 0.5 W to 8 W. **(c)** Maximum temperature change of a 1 μl DI water droplet versus power with different transmission distance, from 1 mm to 10 mm. **(d)** Experimental data and fitted curve of the maximum temperature change versus distance at the fixed input power of 8 W.

D. SIMULATED AND MEASURED RESULTS

Equation (7) demonstrates that the droplet is heated and mixed simultaneously and the temperature distribution is uniform within a very short time.

The heating performance of the SMR in water is simulated by finite element analysis (COMSOL) according to (6) and (7), as shown in figure 2 (a). The wireless heating capacity was investigated with water droplets at different input power as well as transmission distance. To characterize the acoustic heating, the droplet temperature was measured with an inserted thermocouple. All of the experiments were carried out at 20 °C. Figure 2 (b) shows the temperature profiles of a 1 μl water droplet under the stimulation of various input power from 0.5 W to 8 W, while the transmission distance was fixed at 6 mm. The temperature increases during the initial 10 s. The heating rates are calculated to be 0.5, 1.0, 2.2, 3.0 and 3.7 °C /s for the input power

of 0.5, 1.0, 2.0, 4.0 and 8.0 W respectively. After 10 s stimulation, the temperature reaches to a relatively steady state, which is compatible to the results of droplet heating using wire-connected SMR. Here, we also provide the comparison of the expected theoretical curve and the measured heating profile (see supplementary material Figure S4). The input power of the experiment is 8 W and the distance is 6 mm. It is rather difficult to build the simulation model of wireless heating system. Thus, we directly apply the power of receiving antenna with 251 mW, which is calculated by the input power (8 W) multiplied by the efficiency of power transfer from transmitting antenna to receiving antenna (3.14% in this case). The differences between theoretical and experimental curves could be induced by many reasons, for example the liquid volatilization, impedance mismatch and environmental interface. In addition, the temperature change of the water droplet is also dependent with the transmission distance according to (3) and (5). As the transmission distance changing from 1 mm to 10 mm (Figure 2 (c)), the maximum temperature is negatively correlated to the distance, ranging from 60 °C at 1 mm to 16 °C at 10 mm. The experimental data of the maximum temperature change versus transmission distance at the fixed input power of 8 W is plotted in Figure 2 (d). In the case of near field, the maximum temperature change can be fitted by the function of

$$\Delta T = \frac{a}{(x + 10)^5}, \tag{8}$$

Here a is the fitted parameter, and x represented the nearest distance between antennas. Thus, the distance between antennas is the sum of x and antennas' radii. The length of 10 mm represents the sum of antennas' radii. Equation (8) is deduced by (3). The fitting result is well matched with the theory described above (Figure 2(d)). And the differences between experimental and fitted curves are caused by the liquid volatilization, heat conduction of droplet, etc.

In our developed wireless controlled micro-reactor system thorough microscale acoustic devices, some of the energy is converted to heat and some of the energy is used to mix the droplet. Thus, the heating efficiency of our wireless controlling system is less efficient comparable to microwave, induction and LC circuit heating. The heating efficiency of our system is presented in supplementary material (page 3). As the mixing of the droplet is the challenging issue and plays a very important role for improving the reaction efficiency in droplets. We believe our system has the advantages compared with the microwave, induction or LC circuit which cannot achieve local mixing of the droplets.

As predicted by the theory, the mixing rate is also related with the input power and the transmission distance. A series of mixing experiments were then applied. One drop of quantum dots (QDs, CdSSe/ZnS Water Soluble, PL 600 nm) solution was introduced to the water droplet to facilitate the monitoring of the mixing process. Figure 3 (a) shows that when no input power was added to the SMR, the fluorescence
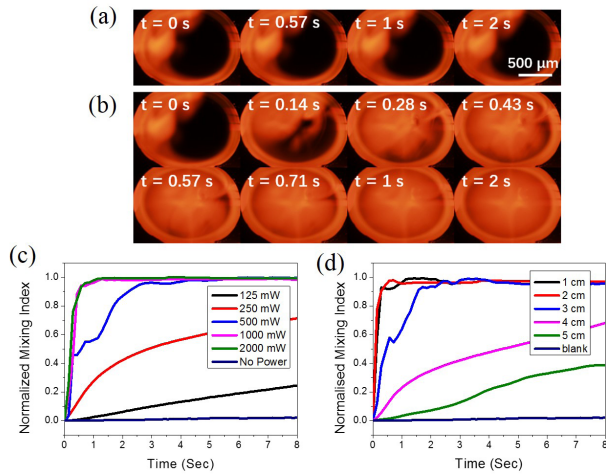
FIGURE 3. Fluorescent microscope images showing the mixing of quantum dot solution and water droplet (a) without input power and (b) with input power at 2 W and fixed wireless transmission distance at 1 cm. (c-d) Normalized mixing index as a function of time with (c) different input power (fixed distance 1 cm) and (d) different distance (fixed input power 8 W). Blank group refers to an infinite distance.

FIGURE 4. (a) Schematic diagram of the H-shaped SMR array integrated with a single antenna. (b) The electric field distribution nearby on integrated PCB board, while the color-bar represents the normalized electric field intensity. Temperature change (c) and normalized mixing index (d) of the four droplets located on top of the SMRs.

distribution remained almost unchanged within 2 s, which is due to the slow diffusion by the Brownian motion. Whereas, when applying power, vigorous multiple micro-vortices were generated immediately in the droplet, leading to a rapid mixing within the droplet (see Figure 3 (b) and the supplementary Video 1).
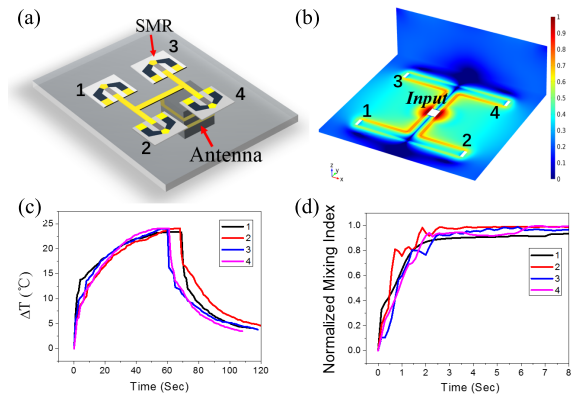
To quantify the mixing efficiency, the normalized mixing index (*NMI*) is introduced. [27], [28] (see supplementary material). Experimental results demonstrated that the NMI is related to the input power (Figure 3 (c)) as well as the transmission distance (Figure 3 (d)). *NMI* increases quickly from 0 to 0.9, within 0.5 s with the input power at 1 W and fixed distance at 1 cm, or within 0.3 s with the distance over 2 cm and fixed input power at 8 W, which both guarantee an effective mixing in the droplet.

III. CIRCUITS DESIGN

A unique advantage to have the wireless controlled heating and mixing is the capability to achieve multiple droplets manipulations. To demonstrate this, two kinds of SMR arrays with H-shaped and rake-shaped circuits were applied respectively.

A. H-SHAPED CIRCUIT

For the H-shaped circuit, an array of four identical 2.5 GHz SMR actuators were placed on the circuit board and connected to the receiving antenna which is located at the center of the board. Figure 4 (a) shows the schematic diagram of the H-shaped wireless SMR array, which consists of one single antenna and four SMRs in parallel connection. The symmetrical circuit structure ensures the symmetrical distribution of electromagnetic field in space. Figure 4 (b) shows the simulated distribution of the electric field on the integrated PCB board which indicates the uniform distribution of

the energy. Thus, the four SMRs will have the same heating and mixing efficiency. Experimentally, the heating rate and mixing index of the four SMRs were measured respectively, under the same stimulations. Experimental results prove that the rather homogeneity droplet heating (Figure 4 (c)) and mixing (Figure 4 (d)) by the four SMRs. The maximum temperature changes of the four SMRs are 23.4, 24.1, 24 and 24.1 °C respectively (under the stimulation of fixed input power of 8 W and transmission distance of 4 mm). The error of the maximum temperature is less than 1 °C. While the normalized mixing index of the four SMRs all increased above 0.8 within 1.5 s under the input power of 2 W and transmission distance fixed at 1 cm. Thus, the wireless H-shaped SMR array can be potentially applied for high-throughput multiple droplets uniform heating and mixing.

B. RAKE-SHAPED CIRCUIT

Besides the uniform heating, non-uniform heating the multi-droplets was also demonstrated by redesigning the circuit. A rake-shaped circuit with five ports arranged in parallel was applied to connect five individual SMRs with the receiving antenna (Figure 5(a)). In this case, the electromagnetic field propagates mainly in the gaps (insulation medium) between the rake-shaped conductor and external ground conductor plane, which will result a non-uniform distribution of the electromagnetic field: strongest electromagnetic field exists on both sides and weakest one exists in the middle. Therefore, the two actuators arranged on both sides (port 1 and 5) will get the most energy while the SMR in the middle (port 3) get the least energy. The remaining two actuators (port 2 and 4) will get the energy between the most and the least. This rake-shaped design of the circuit provides the possibilities to realize a temperature gradient in the droplet array. According to the nature of electromagnetic wave propagation in air (Maxwell equations) and the boundary conditions on the conductor, the distribution of electromagnetic field in space containing such a circuit was solved through
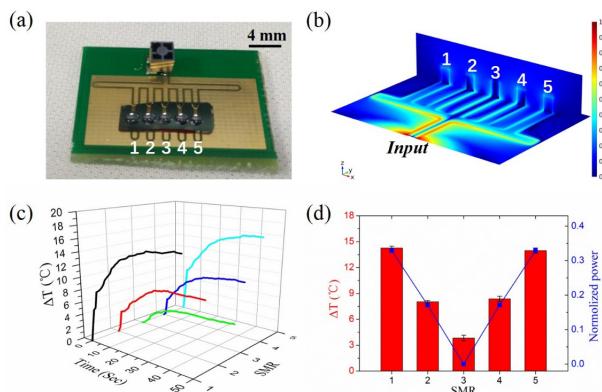
FIGURE 5. (a) Photo of the rake-shaped SMR array integrated with a single antenna. (b) The simulated electric field distribution on the integrated PCB board, while the color-bar represents the normalized electric field intensity. (c) Temperature change of five droplets heated by different SMRs with the fixed input power of 8 W and transmitting distance of 4 mm. (d) Plot of the maximum temperature changes of the five droplets and the normalized power distribution of the five ports calculated by COMSOL.

numerical calculation by COMSOL. Figure 5 (b) shows the simulated distribution of the electric field on the integrated PCB board. The solution domain of electric field in the simulation model is shown in supplementary material (Figure S5). The results indicate that the distribution of electric field with the five ports is non-uniform: port 1 and 5 are the strongest and port 3 is the weakest. It proves the theory analysis above. The different power distribution of the five SMRs will result different vibration intensity and heating efficiency of these SMRs (see supplementary material Video 2). Figure 5 (c) plots the real-time temperature profile of the droplets heated by the five actuators with the fixed input power at 8 W and transmitting distance of 4 mm. It shows that the heating efficiency of the two SMRs on both sides is the highest and the middle one is the lowest, which further demonstrates the theory analysis and simulation results. The maximum temperature changes of these SMRs is shown in Figure 5 (d) and the temperature differences between adjacent SMRs are almost the same (about 5 °C). Besides, finite element analysis gives the transmission coefficients (Scattering parameters) in 2.5 GHz from input (antenna) port to SMR ports. Thus we can evaluate the power applied to each SMR port, which is proportional to the square of transmission coefficient. The normalized power distribution of these SMR ports is shown in Figure 5(d) and consistent with the gradient of the maximum temperature changes. Also, this theoretical power distribution is well matched with the experimental result (see supplementary material Figure S6).
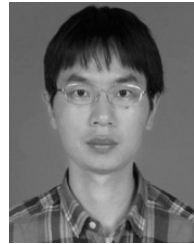
IV. CONCLUSION

In conclusion, for the first time, wireless controlled MEMS piezoelectric resonator array for heating and mixing of multiple liquid droplets is demonstrated. An equivalent circuit model is proposed to describe the wireless coupling and the mechanism of the heating and mixing by SMR. The system performs a heating rate up to 3.7 °C /s and a rapid mixing within 0.3 s in the water droplet. The heating and mixing can be further tuned by adjusting the input power or the wireless transmission distance. Both uniform and non-uniform (gradient) wireless heating of multiple droplets were demonstrated by applying H-shaped and rake-shaped arranged SMR array, which shows great potential as a versatile platform for developing high-throughput micro-reactors.

REFERENCES

[1] P. S. Dittrich and A. Manz, "Lab-on-a-chip: Microfluidics in drug discovery," *Nature Rev. Drug Discovery*, vol. 5, no. 3, pp. 210–218, Mar. 2006.

[2] C. Petucci, J. Diffendal, D. Kaufman, B. Mekonnen, G. Terefenko, and B. Musselman, "Direct analysis in real time for reaction monitoring in drug discovery," *Anal. Chem.*, vol. 79, no. 13, pp. 5064–5070, 2007.

[3] J. J. Agresti *et al.*, "Ultrahigh-throughput screening in drop-based microfluidics for directed evolution," *Proc. Nat. Acad. Sci.*, vol. 107, no. 9, pp. 4004–4009, 2010.

[4] A. Bellomo *et al.*, "Rapid catalyst identification for the synthesis of the pyrimidinone core of HIV integrase inhibitors," *Angewandte Chem. Int. Ed.*, vol. 51, no. 28, pp. 6912–6915, Jul. 2012.

[5] C.-M. Lin, T.-T. Yen, V. V. Felmetsger, M. A. Hopcroft, J. H. Kuypers, and A. P. Pisano, "Thermally compensated aluminum nitride Lamb wave resonators for high temperature applications," *Appl. Phys. Lett.*, vol. 97, no. 8, p. 083501, Aug. 2010.

[6] C.-Y. Lee, W. Pang, H. Yu, and E. S. Kim, "Subpicoliter droplet generation based on a nozzle-free acoustic transducer," *Appl. Phys. Lett.*, vol. 93, no. 3, p. 034104, 2008.

[7] S. J. Widdis, K. Asante, D. L. Hitt, M. W. Cross, W. J. Varhue, and M. R. McDevitt, "A MEMS-based catalytic microreactor for a H_2O_2 monopropellant micropropulsion system," *IEEE/ASME Trans. Mechatronics*, vol. 18, no. 4, pp. 1250–1258, Aug. 2013.

[8] A. Koyama, S. Kawahata, M. Deng, and S. Wakitani, "Operator based fault detection and isolation for microreactor actuated by Peltier devices," in *Proc. IEEE 12th Int. Conf. Netw., Sens. Control (ICNSC)*, Apr. 2015, pp. 191–196.

[9] J. J. Shah *et al.*, "Microwave dielectric heating of fluids in an integrated microfluidic device," *J. Micromech. Microeng.*, vol. 17, no. 11, p. 2224, 2007.

[10] C. Hutter, K. Sefiane, T. Karayiannis, A. Walton, R. Nelson, and D. Kenning, "Nucleation site interaction between artificial cavities during nucleate pool boiling on silicon with integrated micro-heater and temperature micro-sensors," *Int. J. Heat Mass Transf.*, vol. 55, no. 11, pp. 2769–2778, 2012.

[11] V. Studer, A. Pépin, Y. Chen, and A. Ajdari, "An integrated AC electrokinetic pump in a microfluidic loop for fast and tunable flow control," *Analyst*, vol. 129, no. 10, pp. 944–949, 2004.

[12] B. Ivorra, J. L. Redondo, A. M. Ramos, and J. G. Santiago, "Design sensitivity and mixing uniformity of a micro-fluidic mixer," *Phys. Fluids*, vol. 28, no. 1, p. 012005, 2016.

[13] H. Qu *et al.*, "On-chip integrated multiple microelectromechanical resonators to enable the local heating, mixing and viscosity sensing for chemical reactions in a droplet," *Sens. Actuators B, Chem.*, vol. 248, pp. 280–287, Sep. 2017.

[14] H. Zhang *et al.*, "Label-free detection of protein-ligand interactions in real time using micromachined bulk acoustic resonators," *Appl. Phys. Lett.*, vol. 96, no. 12, p. 123702, 2010.

[15] J. Friend and L. Y. Yeo, "Microscale acoustofluidics: Microfluidics driven via acoustics and ultrasonics," *Rev. Mod. Phys.*, vol. 83, pp. 647–704, Jun. 2011.

[16] W. Cui *et al.*, "Localized ultrahigh frequency acoustic fields induced micro-vortices for submilliseconds microfluidic mixing," *Appl. Phys. Lett.*, vol. 109, no. 25, p. 253503, 2016.

[17] Y. Satoh, T. Nishihara, T. Yokoyama, M. Ueda, and T. Miyashita, "Development of piezoelectric thin film resonator and its impact on future wireless communication systems," *Jpn. J. Appl. Phys.*, vol. 44, no. 5R, p. 2883, 2005.

[18] M. Nirschl, M. Schreiter, and J. Vörös, "Comparison of FBAR and QCM-D sensitivity dependence on adlayer thickness and viscosity," *Sens. Actuators A, Phys.*, vol. 165, no. 2, pp. 415–421, 2011.

[19] H. Zhao *et al.*, "Microchip based electrochemical-piezoelectric integrated multi-mode sensing system for continuous glucose monitoring," *Sens. Actuators B, Chem.*, vol. 223, pp. 83–88, Feb. 2016.

[20] T. Thorsen, S. J. Maerkl, and S. R. Quake, "Microfluidic large-scale integration," *Science*, vol. 298, no. 5593, pp. 580–584, 2002.

[21] M. Brivio, W. Verboom, and D. N. Reinhoudt, "Miniaturized continuous flow reaction vessels: Influence on chemical reactions," *Lab Chip*, vol. 6, no. 3, pp. 329–344, 2006.

[22] K. F. Jensen, "Microreaction engineering—Is small better?" *Chem. Eng. Sci.*, vol. 56, no. 2, pp. 293–303, 2001.

[23] D. Issadore, K. J. Humphry, K. A. Brown, L. Sandberg, D. A. Weitz, and R. M. Westervelt, "Microwave dielectric heating of drops in microfluidic devices," *Lab Chip*, vol. 9, no. 12, pp. 1701–1706, Jun. 2009.

[24] S. K. Baek, J. Min, and J. H. Park, "Wireless induction heating in a microfluidic device for cell lysis," *Lab Chip*, vol. 10, no. 7, pp. 909–917, Apr. 2010.

[25] P. S. Chee, M. Nafea, P. L. Leow, and M. S. M. Ali, "Thermal analysis of wirelessly powered thermo-pneumatic micropump based on planar LC circuit," *J. Mech. Sci. Technol.*, vol. 30, no. 6, pp. 2659–2665, 2016.

[26] X. Chen, L. Song, B. Assadsangabi, J. Fang, M. S. M. Ali, and K. Takahata, "Wirelessly addressable heater array for centrifugal microfluidics and *Escherichia coli* sterilization," in *Proc. 35th Annu. Int. Conf. IEEE Eng. Med. Biol. Soc. (EMBC)*, Jul. 2013, pp. 5505–5508.

[27] H. Van Phan, M. B. Coşkun, M. Şeşen, G. Pandraud, A. Neild, and T. Alan, "Vibrating membrane with discontinuities for rapid and efficient microfluidic mixing," *Lab Chip*, vol. 15, no. 21, pp. 4206–4216, 2015.

[28] T.-D. Luong, V.-N. Phan, and N.-T. Nguyen, "High-throughput micromixers based on acoustic streaming induced by surface acoustic wave," *Microfluidics Nanofluidics*, vol. 10, no. 3, pp. 619–625, 2011.

ZHAN WANG received the B.E. degree from Chongqing University, Chongqing, China, in 2015. He is currently a Graduate Student with Tianjin University. His research interests include drug delivery, wireless actuators platforms, and the interaction of nanoparticles (e.g., nanorods) with lipids or cells.

HONGXIANG ZHANG received the B.S. degree from Tianjin University, Tianjin, China, in 2013, where he is currently pursuing the Ph.D. degree. His research interests include acoustic field and waves, nonlinear acoustic effects, and multi-physics field analysis.

YANG YANG received the B.S. degree from Chongqing University, Chongqing, China, in 2015. He is currently pursuing the master's degree with Tianjin University. His research interests focus on microfluidics for the cellular level analysis of diseases, the rapid capture of circulating tumor cell, and drug delivery though hypersonic sound.

HEMI QU received the B.S. and M.S. degrees from Hunan University, Changsha, China, in 2004 and 2007, respectively, and the Ph.D. degree in chemistry from the National University of Singapore, Singapore. He is currently an Assistant Professor with Tianjin University, China. His research interests focus on sensitive material for gas sensors and instrumental miniaturization.
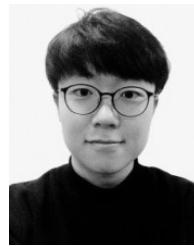
ZIYU HAN received the B.S. degree from Tianjin University, Tianjin, China, in 2014, where he is currently pursuing the Ph.D. degree. His research interests focus on the developments of microfluidic systems and point-of-care devices towards the analysis of biomolecular interactions.

WEI PANG received the B.S. degree from Tsinghua University, Beijing, China, in 2001, and the Ph.D. degree in electrical engineering from the University of Southern California, Los Angeles, CA, USA, in 2006. He was with the Wireless Semiconductor Division, Avago Technologies, Fort Collins, CO, USA. He is currently a Professor with the College of Precision Instrument and Optoelectronics Engineering, Tianjin University, China. His research focuses on the areas of MEMS for RF wireless communications, biological detection, wireless sensor platforms, and medical ultrasound.

XUEXIN DUAN received the B.S. and M.S. degrees from Nankai University, Tianjin, China, in 2001 and 2004, respectively, and the Ph.D. degree from the University of Twente, Enschede, The Netherlands, in 2010. He was with the Max-Planck Institute for Polymer Research, Mainz, Germany, for one year. From 2010 to 2013, he was with Yale University as a Post-Doctoral Researcher. He is currently a Professor with Tianjin University. His research focuses on micro/nano fabricated devices and their applications in chemical or biomolecular sensing.

• • •